DNA Methylation Is Associated with Altered Gene Expression in AMD

Allan Hunter,[1] *Paul A. Spechler,*[1] *Alyssa Cwanger,*[1] *Ying Song,*[1] *Zhe Zhang,*[2] *Gui-shuang Ying,*[3] *Anna K. Hunter,*[2] *Edwin deZoeten,*[4] *and Joshua L. Dunaief*[1]

Purpose. Age-related macular degeneration (AMD) is the leading cause of blindness in the elderly. Evidence suggests oxidative stress plays a role in the disease. To assess the potential contribution of epigenetic regulation of antioxidant genes relevant to AMD pathogenesis, we evaluated DNA methylation, a tissue-specific genetic modulation that affects gene expression.

Methods. Using the Infinium HumanMethylation27 Illumina platform, we performed DNA bisulfite sequencing to compare the methylation status in postmortem retina pigment epithelium (RPE)/choroid between patients with AMD and age-matched controls. Gene expression was assessed with the Affymetrix Exon Array. TaqMan gene expression assays were used for relative quantification (RT-PCR) confirmation of the expression array results. Glutathione S-transferase isoform mu1 (*GSTM1*) and mu5 (*GSTM5*) promoter methylation was confirmed by CpG island bisulfite pyrosequencing. To assess protein levels and localization, we used Western analysis, immunohistochemistry, and immunofluorescence with murine and human samples.

Results. The mRNA levels of *GSTM1* and *GSTM5* were significantly reduced in AMD versus age-matched controls in RPE/choroid and neurosensory retina (NSR), which corresponded to hypermethylation of the *GSTM1* promoter. mRNA and protein levels were decreased (RPE to a greater extent than NSR) in AMD postmortem samples, irrespective of age. Immunohistochemistry and immunofluorescence confirm the presence of the enzymes in the NSR and RPE.

Conclusions. Comparison of DNA methylation, together with mRNA levels, revealed significant differences between AMD versus normal retinas. The evidence presented suggests that *GSTM1* and *GSTM5* undergo epigenetic repression in AMD

RPE/choroid, which may increase susceptibility to oxidative stress in AMD retinas. (*Invest Ophthalmol Vis Sci.* 2012; 53:2089–2105) DOI:10.1167/iovs.11-8449

The retina's high oxygen saturation and easily oxidized polyunsaturated fatty acids (e.g., docosahexaenoate [DHA]) impart a great oxidative burden.[1-3] These oxidative insults can cause irreversible damage to retinal cellular machinery and function.[4-7] Mechanisms used to counter oxygen toxicity include compartmentalization, repair, removal of damaged macromolecules, and free radical elimination by "scavenger" molecules, such as vitamins or antioxidant enzymes or compounds.[8,9]

Although the cause of age-related macular degeneration (AMD) is not completely understood, there is evidence that oxidative stress is involved. Antioxidant vitamins can slow the progression in moderate to advanced AMD.[10] The retina has a high concentration of vitamin C, a natural antioxidant, which decreases after intense light exposure.[11,12] The choroidal arteries have the highest oxygen saturation in the body.[13,14] There is an increase in ω-(2-carboxyethyl)pyrrole protein adducts secondary to oxidation of DHA-containing lipids in the retinas in AMD versus controls.[15,16]

These oxidative insults cause an accumulation of free radical by-products. In addition, patients with AMD appear to have a reduced serum antioxidant potential, which is partially alleviated by vitamin supplementation.[16,17] Further, smoking, a potent oxidative insult, is a known risk factor for AMD.[18-22]

More than solely damaging proteins and lipids, free radicals can influence chromatin structure. Oxygen radicals can cause point mutations, deletions, and rearrangements.[23,24] One result is altered sequence-specific-protein interactions. DNA methyl transferases (DNMTs), for example, when confronted with free radical induced DNA damage, change the methylation "profile" of DNA. Indeed, reactive oxygen species have been shown to cause both hyper- and hypomethylation of DNA.[25,26]

The modification of DNA by the addition of a methyl group to cytosine changes the electrostatic nature of chromatin.[27,28] DNA methylation, along with histone acetylation, deacetylation, or methylation, is a primary chemical modification that alters transcription factor–DNA affinity. Hypermethylation of promoter CpG islands and further upstream cis-regulatory CpG "island shores" have been linked with heterochromatin and gene silencing.[29-34] The methylated cytosines of DNA act, primarily, by increasing electrostatic interactions with methyl-CpG-binding domain (MBD) proteins that act as transcriptional repressors through interactions with histone deacetylases (HDACs).

Decreased expression of glutathione S-transferase phi (GSTP1) has been linked to DNA hypermethylation in certain cancers, and mRNA levels are diminished in AMD.[35,36] GSTP1 is a scavenger of reactive oxygen species and its absence could

TABLE 1. A Total of 46 mRNAs from the Affymetrix Exon Microarray That Showed a Significant Correlation ($P < 0.1$) Between HCS and NDRI Samples and Also Had an FC of More Than 25% Between AMD and Control

Gene_ID	Chr	Symbol	HCS					NDRI					Name
			Control	AMD	AMD-Control	FC	NSD	Control	AMD	AMD-Control	FC	P Value	
10,930	6	APOBEC2	4.749	6.450	1.701	3.250	3.154	6.245	6.665	0.420	1.338	0.028	Apolipoprotein B mRNA editing enzyme, catalytic polypeptide-like 2
6228	5	RPS23	8.039	9.413	1.374	2.591	9.466	9.490	9.872	0.382	1.303	0.011	Ribosomal protein S23
4160	18	MC4R	3.121	4.339	1.217	2.325	3.855	4.673	5.494	0.821	1.767	0.045	Melanocortin 4 receptor
100,132,476	17	KRTAP4-7	7.174	8.324	1.150	2.219	3.846	7.532	7.886	0.353	1.278	0.099	Keratin-associated protein 4-7
100,129,026		NA	6.507	7.454	0.947	1.928	5.516	7.487	7.880	0.393	1.313	0.010	NA
731,157	5	LOC731157	4.550	5.289	0.740	1.670	3.731	5.198	5.650	0.452	1.368	0.025	Similar to HSPC101
730,032	2	LOC730032	5.110	5.663	0.553	1.467	3.468	5.143	5.629	0.486	1.400	0.012	Similar to RIKEN cDNA C230030N03
729,851		NA	3.784	4.330	0.546	1.460	3.521	4.207	4.731	0.524	1.438	0.036	NA
79,870	8	BAALC	6.009	6.509	0.499	1.414	6.270	6.931	7.365	0.435	1.352	0.079	Brain and acute leukemia, cytoplasmic
284,120		NA	5.413	5.768	0.355	1.279	3.973	5.973	6.507	0.534	1.448	0.067	NA
4482	8	MSRA	8.481	8.134	-0.347	-1.272	5.486	7.965	7.635	-0.330	-1.257	0.019	Methionine sulfoxide reductase A
340,371	8	NRBP2	9.481	9.098	-0.382	-1.303	3.880	8.832	8.389	-0.444	-1.360	0.022	Nuclear receptor binding protein 2
2844	9	GPR21	7.854	7.422	-0.432	-1.349	4.245	7.618	7.091	-0.527	-1.441	0.042	G protein-coupled receptor 21
100,131,601	16	LOC100131601	7.031	6.587	-0.444	-1.360	3.136	6.541	6.121	-0.420	-1.338	0.031	Similar to hCG1980470
29,065	8	DDEF1IT1	6.723	6.268	-0.455	-1.371	3.061	6.207	5.819	-0.388	-1.308	0.006	DDEF1 intronic transcript 1 (nonprotein coding)
100,131,231	9	LOC100131231	8.344	7.871	-0.473	-1.388	4.176	8.077	7.741	-0.336	-1.262	0.057	Hypothetical protein LOC100131231
58,496	6	LY6G5B	8.878	8.394	-0.484	-1.398	7.390	8.683	8.331	-0.352	-1.276	0.055	Lymphocyte antigen 6 complex, locus G5B
729,793		NA	7.227	6.714	-0.513	-1.427	4.324	6.689	6.271	-0.418	-1.336	0.047	NA
55,556	18	ENOSF1	8.999	8.484	-0.515	-1.429	3.166	8.554	8.113	-0.441	-1.357	0.010	Enolase superfamily member 1
645,771	13	RP11-385E5.2	3.482	2.937	-0.546	-1.460	3.453	3.571	3.171	-0.400	-1.320	0.015	Poly (ADP-ribose) polymerase family, member 4 pseudogene
642,367		NA	6.605	6.057	-0.548	-1.462	8.032	6.085	5.746	-0.339	-1.265	0.022	NA
100,129,743	2	RPL7P14	6.644	6.086	-0.558	-1.472	14.077	5.712	4.947	-0.766	-1.700	0.007	Ribosomal protein L7 pseudogene 14
6819	2	SULT1C2	8.329	7.725	-0.604	-1.520	5.642	7.492	6.955	-0.538	-1.452	0.036	Sulfotransferase family, cytosolic, 1C, member 2
728,655	6	HULC	5.293	4.674	-0.619	-1.536	3.010	5.123	4.677	-0.446	-1.362	0.008	Highly upregulated in liver cancer (nonprotein coding)
388,815	21	C21orf34	8.434	7.807	-0.627	-1.545	4.506	7.900	7.342	-0.558	-1.472	0.055	Chromosome 21 open reading frame 34
646,272	4	LOC646272	4.966	4.336	-0.630	-1.547	3.221	4.613	4.283	-0.329	-1.257	0.019	Similar to ubiquinol-cytochrome c reductase, complex III subunit VII

TABLE 1. Continued

Gene_ID	Chr	Symbol	HCS					NDRI					Name
			Control	AMD	AMD-Control	FC	NSD	Control	AMD	AMD-Control	FC	P Value	
8038	10	ADAM12	7.512	6.861	−0.652	−1.571	5.172	6.763	6.400	−0.363	−1.286	0.091	ADAM metallopeptidase domain 12
100,130,696		NA	4.040	3.385	−0.655	−1.575	4.061	3.907	3.494	−0.413	−1.331	0.043	NA
727,819		NA	4.729	4.069	−0.660	−1.580	3.915	4.228	3.722	−0.506	−1.420	0.017	NA
51,134	12	CCDC41	5.660	4.955	−0.705	−1.630	5.269	5.475	5.143	−0.332	−1.259	0.019	Coiled-coil domain containing 41
10,693	17	CCT6B	4.769	4.037	−0.731	−1.660	5.336	4.632	4.244	−0.388	−1.308	0.046	Chaperonin containing TCP1, subunit 6B (zeta 2)
51,474	12	LIMA1	9.444	8.673	−0.771	−1.706	3.632	9.245	8.895	−0.350	−1.275	0.070	LIM domain and actin binding 1
100,131,993	13	LOC100131993	7.989	7.170	−0.819	−1.764	3.880	6.957	6.556	−0.401	−1.321	0.077	Similar to hCG2020760
2949	1	GSTM5	9.389	8.444	−0.946	−1.926	2.102	9.117	8.622	−0.495	−1.409	0.037	Glutathione S-transferase mu 5
28,516	14	TRDV3	5.083	4.076	−1.007	−2.010	4.140	4.386	3.926	−0.460	−1.376	0.069	T-cell receptor delta variable 3
5729	14	PTGDR	7.864	6.839	−1.024	−2.034	3.878	7.302	6.727	−0.575	−1.490	0.064	Prostaglandin D2 receptor (DP)
5935	X	RBM3	9.893	8.865	−1.028	−2.040	6.851	9.693	8.963	−0.730	−1.659	0.100	RNA binding motif (RNP1, RRM) protein 3
10,561	1	IFI44	7.002	5.951	−1.051	−2.072	9.181	6.777	6.083	−0.694	−1.618	0.093	Interferon-induced protein 44
100,132,099	13	UNQ1829	6.932	5.777	−1.155	−2.227	4.265	6.116	5.494	−0.622	−1.539	0.038	FRSS1829
100,129,349	1	IFI44L	7.324	6.026	−1.299	−2.460	5.245	7.029	6.375	−0.654	−1.574	0.070	NA
440,482	18	ANKRD20A5	6.053	4.751	−1.302	−2.466	3.087	5.492	4.416	−1.076	−2.108	0.040	Ankyrin repeat domain 20 family, member A5
391,267	21	C21orf81	7.626	6.062	−1.563	−2.956	4.678	6.672	5.774	−0.898	−1.864	0.004	Ankyrin repeat domain 20 family, member A3 pseudogene
390,072	11	OR52N4	6.241	4.655	−1.586	−3.002	4.645	6.035	5.351	−0.685	−1.608	0.051	Olfactory receptor, family 52, subfamily N, member 4
284,232	13	LOC284232	5.678	4.034	−1.644	−3.125	5.628	4.465	3.538	−0.926	−1.901	0.001	Ankyrin repeat domain 20 family, member A2 pseudogene
80,867	6	HCG2P7	6.870	4.550	−2.320	−4.995	9.852	5.120	4.420	−0.700	−1.625	0.045	HLA complex group 2 pseudogene 7
2944	1	GSTM1	10.748	6.768	−3.980	−15.780	3.376	8.688	5.950	−2.738	−6.672	0.002	Glutathione S-transferase mu 1

List is ordered by decreasing FC for the HCS samples. Chr, chromosome.

reduce protection from genome-damaging oxidants, resulting in increased vulnerability to further oxidative insults.

Although DNA methylation is an inheritable, covalent epigenetic change, it is modifiable. "Silenced' expression can be increased with demethylation of the promoter region.[37,38] The demethylation activity of the spice curcumin and the phenol epigallocatechin-3-gallate, found in green tea, has been described.[39-41] Green tea polyphenols inhibit DNMT1 in human prostate cancer cells, resulting in demethylation of the proximal GSTP1 promoter and increased expression of GSTP1.[42]

AMD phenotype discordance in monozygotic (MZ) twins helps clarify the potential impact of environment on AMD pathogenesis, given MZ twins' identical genetic background. Worse AMD phenotype (i.e., advanced stage of disease and fundoscopy with larger drusen size and/or pigment area) was associated with the MZ twin who smoked the most and had the lower dietary intake of vitamin D, betaine, and methionine. These modifiable environmental and dietary exposures have been shown to effect DNA methylation and epigenetic mechanisms.[43]

To determine if DNA methylation is involved in gene expression in AMD, we used microarray technology. Herein, we detected expression differences in AMD versus age-matched controls using the Affymetrix exon microarray in postmortem retina pigment epithelium (RPE)/choroid samples. Coupling expression results to DNA bisulfite sequencing with the Infinium HumanMethylation27 Illumina array (San Diego, CA) showed a significant methylation change of promoter CpG sites that corresponded to altered expression of 63 genes.

MATERIALS AND METHODS

Histopathologic Assessment

Whole human donor eyes were obtained from the National Disease Research Interchange (NDRI, Philadelphia, PA) and whole human RPE/choroid were from Christine Curcio (University of Alabama, Birmingham, AL). All specimens were obtained in accordance with institutional review board regulations and the provisions of the Declaration of Helsinki for research involving human tissues (Supplemental Table 1, available at http://www.iovs.org/lookup/suppl/doi:10.1167/iovs.11–8449/-/DCSupplemental). Average postmortem tissue harvest time was 5.2 hours (range 2.5 to 9.0 hours).

Specimen Preparation

The postmortem specimens were flash frozen upon tissue harvest and stored in −70°C at all times. Tissue preparation was done on dry ice. The anterior segments were removed. The posterior segment of the eye was cut into quarters centered upon the fovea and the horizontal section was placed through the horizontal raphe of the retina and the optic nerve center. The neurosensory retina (NSR) and RPE/choroid were then separated.

DNA and RNA isolation

DNA isolation was performed with the DNeasy Blood & Tissue Kit (Qiagen, Inc., Germantown, MD) per manufacturer's protocol. The final DNA concentration was determined by nanodrop and diluted to 50 ng/μL. RNA was isolated with the RNeasy Mini Kit (Qiagen, Inc.) per manufacturer's protocol. The final RNA concentration was determined by nanodrop and diluted to 50 ng/μL.

DNA Bisulfite Conversion

DNA was bisulfite converted using the EZ DNA Methylation kit (Zymo Research, Irvine, CA) per manufacturer's protocol.

PCR of Bisulfite-Treated DNA to Confirm Conversion

Primers to confirm DNA bisulfite conversion were obtained from EZ DNA Methylation kit (Zymo Research) and PCR was done per manufacturer's protocol.

RNA Analysis on Affymetrix Exon Array

Nanochips were run on Agilent (Santa Clara, CA) Bioanalyzer 2100 to determine the quantity and concentration of RNA. Ambion (Santa Clara, CA) WT Expression Kit for Affymetrix GeneChip Whole Transcript (WT) Expression Arrays, P/N 4425209 was used to generate sense-strand cDNA from 100 ng of total RNA. A 5.5-μg amount of sense-strand cDNA was fragmented and labeled using the Affymetrix (Santa Clara, CA) GeneChip WT Terminal Labeling and Hybridization Kit (PN 702880); 5 μg of fragmented and labeled sense-strand cDNA was hybridized to an Affymetrix HuEx1.0ST Array. Arrays were washed on an Affymetrix GeneChip Fluidics Station 450 using fluidics protocol FS450_0001 and scanned on Affymetrix GeneChip Scanner 3000.

Gene-level measurements were obtained by applying the Robust Multichip Average (RMA) method implemented in the "affy" package of BioConductor to the raw data and using the custom library file generated by BRAINARRAY. The processed data set includes 23,536 unique Entrez genes. The gene-level data of all RPE samples were further normalized by the QSPLINE method also implemented in the "affy" package using autosomal genes.

Illumina Infinium HumanMethylation27 Microarray

High-resolution methylation analyses of AMD eyes ($n = 10$) and normal eyes ($n = 11$) were conducted on the Illumina Infinium Human-Methylation27 microarray platform. This BeadChip assay measures methylation, given as a β value ranging from zero to one, at more than 27,000 CpG loci. Results were outputted by BeadStudio without normalization. Arrays were processed at the Center for Applied Genomics at Children's Hospital of Philadelphia according to the manufacturer's protocol.

Array control probes were used to assess sample performance. Multivariate characteristics of array control probes were used to screen outliers. Sex chromosome loci ($n = 1092$) were excluded to avoid gender-specific methylation bias, resulting in a final dataset that consisted of 26,486 autosomal loci associated with 13,890 genes. Sequence context information such as CpG island status and transcription factor binding site proximity was extracted from tracks of the University of California Santa Cruz Genome Browser (http://genome.ucsc.edu/).

Pyrosequencing

Human glutathione-S-transferase mu1 (*GSTM1*) methylation assays were developed to cover nine CG dinucleotides from −540 to −320 from the translational start site (ATG) based on Ensembl Gene ID Ensembl:ENSG00000134184. To sequence through every CpG site in this region, two PCR reactions and three pyrosequencing assays were designed and tested for PCR preferential amplification and quantitative pyrosequencing. The bisulfate-converted target sequences from each pyrosequencing reaction are listed in Supplemental Table 2 (available at http://www.iovs.org/lookup/suppl/doi:10.1167/iovs.11–8449/-/DCSupplemental).

Human glutathione-S-transferase mu5 (*GSTM5*) methylation assays were developed to cover 32 CG dinucleotides −577 to −16 from the translational start site (ATG) based on Ensembl Gene ID Ensembl:ENSG00000134201. To sequence through every CpG site in this region, three PCR reactions and five pyrosequencing assays were designed and tested for PCR preferential amplification and quantitative pyrosequencing. Bisulfite-converted target sequences from each pyrosequencing reaction are listed in Supplemental Table 2: ADS1741 is for *GSTM1* promoter and ADS1746 to 1748 are for *GSTM5* promoter.

Bisulfite conversion was carried out as stated previously. PCR was performed with 0.2 μM of each primer and one of the PCR primers was biotinylated to purify the final PCR product using Sepharose beads. The PCR product was bound to streptavidin sepharose HP (Amersham Biosciences, Uppsala, Sweden), and the sepharose beads containing immobilized PCR product were purified, washed, and denatured using a 0.2-M NaOH solution and rewashed using the Pyrosequencing Vacuum Prep Tool (Pyrosequencing, Qiagen), as recommended by the manufacturer. Then, 0.5 μM Pyrosequencing primer was annealed to the purified single-stranded PCR product; 10 μL of the PCR products were sequenced by Pyrosequencing PSQ96 HS System (Pyrosequencing, Qiagen) following the manufacturer's instructions. Methylation status of each locus was analyzed individually as a T/C SNP using QCpG software (Pyrosequencing, Qiagen).

Quantitative Real-Time RT-PCR

Quantitative PCR (qPCR) was done using the TaqMan Custom Array (Applied Biosystems, Carlsbad, CA). RNA isolation/quantification and synthesis of cDNA were done as described.[44] Gene expression assays (TaqMan; Applied Biosystems) were obtained and used for PCR analysis. Genes are listed in Table 2. Eukaryotic 18S rRNA (Hs99999901_s1) served as an internal control. qPCR was performed and results analyzed as described.[44]

Immunohistochemistry

Human postmortem globes were prepared as described.[44] Immunohistochemistry was performed on 10-μm-thick sections, as described.[45] The sections were bleached with the Delicate Melanin Bleach Kit for Special Stains and Immunohistochemistry (IHC) (Polysciences, Inc., Warrington, PA) per manufacturer's protocol. Primary antibodies were rabbit anti-*GSTM1* (Abcam, Cambridge, MA) at 1:2500 dilution and rabbit anti-*GSTM5* (Abcam) at 1:2500 dilution. Control sections were treated identically except for the omission of primary antibodies. Sections were analyzed by bright field microscopy with identical exposure parameters using the Eclipse 80i microscope (Nikon, Melville, NY) with NIS Elements software (Nikon).

Immunofluorescence

Human postmortem globes were prepared as described.[44] Immunofluorescence was performed on 10-μm-thick sections, as described.[46] Primary antibodies were rabbit anti-*GSTM1* (Abcam, Cambridge, MA) at 1:2500 dilution. Primary antibody reactivity was detected using fluorophore-labeled secondary antibodies (Jackson ImmunoResearch Laboratories, West Grove, PA). Control sections and section analysis were done as described above.

Western Analysis

Human postmortem NSR samples were dissected and processed for Western analysis as described.[44] Membranes were incubated overnight at 4°C with rabbit anti-*GSTM1* (Abcam) at 1:1000 dilution and rabbit anti-*GSTM5* (Abcam) antibody at 1:1000 dilution. After washes, membranes were incubated, developed, and imaged as described.[44]

Statistical Analysis

Methylation and gene expression microarray data were analyzed in R statistical software environment v2.11.1 (http://www.r-project.org). The difference between normal and AMD was represented as fold change (FC) and the number of AMD sample standard deviations (NSD) was calculated. Pearson correlation of FCs of the histologically confirmed samples (HCS) and NDRI samples was calculated. One-sided *t*-test was applied to the NDRI samples. Pearson correlation of β difference of the HCS and NDRI samples was calculated. One-sided *t*-test was also applied to the NDRI samples to validate the group differences of HCS samples.

TABLE 2. PCR Analysis (AMD/Control) of Individual RPE/Choroid mRNAs That Were Significantly Increased or Decreased in the Exon Microarray

Gene ID	FC (AMD:Control RPE)	*P* Value
FC confirmation by qPCR of mRNAs originally quantified by the exon microarray		
GSTM1	0.02	< 0.05
GPR21	0.03	< 0.05
LOC10013	0.05	< 0.05
c21orf34	0.33	< 0.05
GSTM5	0.34	< 0.05
RPS23	**0.41**	**NS**
PTGDR	0.46	< 0.05
IF144	0.51	< 0.05
CCT6B	0.63	< 0.05
LY6G5B	0.63	< 0.05
ADAM12	0.65	< 0.05
ARSG	0.65	< 0.05
CCDC41	0.73	< 0.05
NRBP2	0.76	< 0.05
ANGPTL2	0.78	NS
MSRA	0.79	NS
ENOSF1	0.83	NS
SULT1C2	0.86	NS
LIMA1	0.89	NS
BAALC	1.62	< 0.05
MC4R	2.22	< 0.05
APOBEC2	2.97	< 0.05
ALOX15B	3.36	< 0.05
AANAT	3.91	< 0.05
qPCR quantification (AMD versus controls) of mRNAs involved in epigenetic modulation		
MBD1	0.98	NS
MBD2	0.92	NS
MBD3	1.14	NS
MeCP2	1.02	NS
TRDMT1	0.61	NS
HAT1	0.83	NS
HDAC9	0.69	NS
HNMT	0.53	NS

$P < 0.05$ was statistically significant; $P > 0.05$ was NS. All relative expression changes (i.e., increased or decreased) as determined by exon microarray were confirmed by qPCR, except for RPS23, listed in bold type.

Comparison of demographic characteristics between AMD cases and normal controls was performed by Fisher's exact test for categorical characteristics, and two-group *t*-test and Wilcoxon rank sum test for continuous characteristics.

qPCR data in AMD and normal control groups were summarized by mean $\pm$ SE and compared using the two-group *t*-test. The Western quantification data and mRNA data were summarized by median (minimum, maximum) and compared between AMD and normal controls using Wilcoxon rank sum test owing to the skewed distribution of data. Two-sided *P* less than 0.05 was considered statistically significant. These analyses were performed with statistical software GraphPad (GraphPad Software, Inc. San Diego, CA) and SAS v9.2 (SAS Institute Inc., Cary, NC).

RESULTS

Analysis of RPE/Choroid mRNA Levels in AMD Versus Controls by Microarray

Microarray analysis of AMD versus control RPE/choroid samples included 23,536 unique Entrez genes (Supplemental Table 3,

TABLE 3. 67 CpG Sites Determined by Bisulfite Microarray Sequencing of RPE/Choroid That Showed a Significant Correlation ($P < 0.1$) Between HCS and NDRI Samples and Also Had a 5% Methylation Difference Between AMD and Control

Gene ID	Chr	Symbol	CpG	Loc	TSS Coordinate	Distance to TSS	HCS Control	HCS AMD	HCS AMD-Control	HCS NSD	NDRI Control	NDRI AMD	NDRI AMD-Control	P Value
117,194	11	MRGPRX2	cg22051636	19,038,166	19,038,804	638	0.271	0.804	0.534	19.988	0.691	0.802	0.112	0.073
3716	1	JAK1	cg15997411	65,124,972	65,124,574	−398	0.711	0.879	0.168	10.090	0.857	0.878	0.020	0.050
84,221	21	C21orf56	cg07747299	46,428,480	46,428,729	249	0.516	0.143	−0.373	8.264	0.218	0.128	−0.089	0.025
84,699	19	CREB3L3	cg23777956	4,104,671	4,104,629	42	0.487	0.267	−0.220	6.970	0.346	0.300	−0.046	0.054
9724	13	UTP14C	cg24167928	51,496,903	51,496,828	75	0.856	0.918	0.062	6.303	0.871	0.894	0.023	0.041
51,179	1	HAO2	cg03762535	119,713,003	119,712,925	78	0.564	0.637	0.073	6.194	0.632	0.669	0.038	0.090
132,724	4	TMPRSS11B	cg19510180	68,794,175	68,794,004	−171	0.661	0.736	0.074	6.161	0.681	0.709	0.027	0.076
4481	8	MSR1	cg01668126	16,095,111	16,094,595	−516	0.867	0.802	−0.065	6.126	0.859	0.836	−0.022	0.028
284,114	17	TMEM1102	cg14782678	7,280,445	7,279,486	959	0.511	0.455	−0.056	6.011	0.488	0.469	−0.019	0.049
134,864	6	TAAR1	cg15582891	133,008,721	133,008,835	114	0.573	0.731	0.158	6.005	0.726	0.754	0.028	0.030
50,514	9	DEC1	cg26981881	116,943,245	116,943,918	−673	0.761	0.828	0.067	5.359	0.807	0.836	0.029	0.020
29,974	10	ACF	cg03817621	52,315,405	52,315,441	36	0.727	0.844	0.117	4.866	0.789	0.815	0.025	0.061
55,856	6	THEM2	cg16381688	24,773,926	24,775,254	−1328	0.680	0.753	0.073	4.286	0.713	0.738	0.025	0.065
10,507	9	SEMA4D	cg22496652	91,284,445	91,284,431	−14	0.707	0.625	−0.082	4.263	0.672	0.648	−0.024	0.070
6374	4	CXCL5	cg04559909	75,083,589	75,083,280	−309	0.438	0.581	0.143	4.173	0.554	0.593	0.039	0.092
2532	1	DARC	cg23507131	157,440,780	157,441,134	−354	0.698	0.622	−0.076	4.088	0.677	0.652	−0.025	0.048
5478	7	PPIA	cg17269548	44,802,815	44,802,777	38	0.179	0.255	0.076	3.998	0.163	0.207	0.045	0.011
1232	3	CCR3	cg11126313	46,259,266	46,258,692	574	0.785	0.846	0.061	3.991	0.800	0.845	0.044	0.003
83,876	18	MRO	cg27318546	46,599,904	46,600,366	462	0.193	0.128	−0.064	3.829	0.191	0.165	−0.026	0.069
221,823	7	PRPS1L1	cg00911873	18,033,988	18,034,011	23	0.812	0.863	0.051	3.773	0.786	0.842	0.055	0.010
6613	17	SUMO2	cg19776090	70,690,552	70,690,693	141	0.378	0.430	0.053	3.752	0.352	0.376	0.025	0.039
337,977	21	KRTAP21-1	cg22373097	31,050,931	31,049,567	−1364	0.575	0.749	0.174	3.568	0.715	0.787	0.072	0.042
3694	2	ITGB6	cg21105318	160,764,766	160,764,836	70	0.825	0.895	0.070	3.547	0.857	0.881	0.024	0.049
84,218	17	TBC1D3	cg14532417	33,601,782	33,602,396	614	0.813	0.737	−0.076	3.492	0.783	0.751	−0.032	0.069
63,895	18	FAM38B	cg21165219	10,688,044	10,687,814	−230	0.744	0.800	0.055	3.417	0.794	0.821	0.026	0.061
4719	2	NDUFS1	cg06868758	206,733,636	206,732,432	−1204	0.551	0.470	−0.081	3.409	0.456	0.434	−0.022	0.054
54,103	7	LOC54103	cg26594488	76,873,584	76,873,361	−223	0.789	0.858	0.069	3.255	0.797	0.839	0.042	0.023
2044	4	EPHA5	cg13701273	66,218,375	66,218,104	−271	0.136	0.191	0.055	3.120	0.146	0.195	0.049	0.057
260,436	4	C4orf7	cg25600236	71,125,801	71,126,404	−603	0.650	0.750	0.099	3.103	0.746	0.777	0.030	0.061
1184	X	CLCN5	cg20062122	49,720,482	49,720,896	−414	0.842	0.892	0.050	3.063	0.855	0.880	0.025	0.081
390,212	11	GPR152	cg00587613	66,976,799	66,976,776	−23	0.877	0.827	−0.050	3.051	0.857	0.837	−0.020	0.069
79,861	10	TUBAL3	cg07803864	5,436,998	5,436,795	−203	0.748	0.805	0.057	3.039	0.767	0.794	0.028	0.100
10,148	19	EBI3	cg16592658	4,180,887	4,180,540	347	0.748	0.661	−0.087	3.018	0.745	0.712	−0.033	0.032
7531	17	YWHAE	cg25299176	1,250,091	1,250,267	176	0.115	0.210	0.096	3.017	0.126	0.176	0.049	0.079
126,433	19	FBXO27	cg11402505	44,215,038	44,215,276	−238	0.183	0.124	−0.059	3.000	0.155	0.130	−0.025	0.033
1041	6	CDSN	cg24735489	31,196,331	31,196,202	−129	0.729	0.638	−0.091	2.933	0.716	0.692	−0.024	0.038
351	21	APP	cg00542846	26,465,416	26,465,003	−413	0.178	0.234	0.056	2.891	0.210	0.262	0.052	0.059
84,221	21	C21orf56	cg10296238	46,429,602	46,428,729	−873	0.515	0.298	−0.217	2.885	0.385	0.265	−0.120	0.053
3784	11	KCNQ1	cg16465939	2,510,986	2,439,259	71,727	0.149	0.200	0.051	2.847	0.209	0.228	0.019	0.056
339,500	1	ZNF678	cg26683023	225,817,515	225,817,867	−352	0.740	0.794	0.054	2.815	0.757	0.797	0.040	0.009
166,647	4	GPR125	cg26631477	22,126,293	22,126,770	477	0.173	0.245	0.072	2.771	0.168	0.197	0.029	0.054
196,472	12	FAM71C	cg04282622	98,565,053	98,565,662	−609	0.742	0.801	0.059	2.726	0.790	0.823	0.033	0.042
81,493	1	SYNC1	cg05342835	32,933,378	32,933,460	82	0.585	0.452	−0.133	2.668	0.529	0.478	−0.050	0.033
8061	11	FOSL1	cg18818531	65,424,853	65,424,573	−280	0.697	0.595	−0.101	2.649	0.650	0.611	−0.039	0.065

TABLE 3. Continued

Gene ID	Chr	Symbol	CpG	Loc	TSS Coordinate	Distance to TSS	HCS			NSD	NDRI			
							Control	AMD	AMD-Control		Control	AMD	AMD-Control	P Value
388,818	21	KRTAP26-1	cg18822544	30,614,336	30,614,478	142	0.760	0.674	−0.086	2.611	0.727	0.697	−0.030	0.057
8369	6	HIST1H4G	cg23540745	26,355,112	26,355,184	72	0.648	0.717	0.068	2.592	0.647	0.680	0.033	0.050
114,035	21	C21orf81	cg14384940	14,274,661	14,274,636	−25	0.339	0.459	0.121	2.439	0.399	0.497	0.098	0.021
120,065	11	OR5P2	cg13410437	7,774,741	7,775,065	324	0.828	0.886	0.058	2.412	0.882	0.907	0.025	0.024
127,943	1	FCRLM2	cg27495845	159,959,712	159,959,081	631	0.502	0.573	0.072	2.404	0.572	0.617	0.045	0.026
81,793	4	TLR10	cg23855121	38,461,333	38,460,984	−349	0.629	0.684	0.055	2.376	0.663	0.690	0.027	0.072
4848	12	CNOT2	cg10464585	68,922,758	68,923,489	−731	0.218	0.155	−0.064	2.329	0.202	0.161	−0.041	0.100
148,646	1	C1orf188	cg15731815	6,191,847	6,191,507	340	0.170	0.275	0.105	2.313	0.218	0.285	0.068	0.078
284,424	19	C19orf30	cg03996793	4,720,537	4,720,152	385	0.157	0.245	0.088	2.284	0.210	0.252	0.042	0.072
3150	21	HMGN1	cg13791713	39,642,786	39,642,917	131	0.264	0.317	0.053	2.279	0.265	0.291	0.026	0.067
23,524	16	SRRM2	cg06736444	2,741,794	2,742,655	−861	0.317	0.481	0.164	2.262	0.362	0.399	0.037	0.090
3827	3	KNG1	cg12454167	187,917,754	187,917,814	−60	0.492	0.331	−0.162	2.235	0.352	0.305	−0.047	0.071
3624	7	INHBA	cg16415646	41,709,526	41,709,231	−295	0.806	0.865	0.059	2.235	0.819	0.851	0.032	0.046
163,589	1	TDRD5	cg09656934	177,828,123	177,827,648	475	0.214	0.276	0.062	2.189	0.250	0.282	0.032	0.069
27,004	14	TCL6	cg05023540	95,186,723	95,187,268	−545	0.735	0.675	−0.060	2.181	0.734	0.702	−0.032	0.063
3212	17	HOXB2	cg09313705	43,977,490	43,977,391	−99	0.275	0.370	0.095	2.151	0.314	0.344	0.030	0.092
64,174	16	DPEP2	cg04774694	66,590,771	66,590,857	86	0.757	0.696	−0.061	2.124	0.728	0.708	−0.020	0.073
5369	5	PMCHL1	cg12530080	22,177,396	22,178,218	−822	0.683	0.741	0.057	2.119	0.725	0.750	0.024	0.066
9541	2	CIR	cg14138171	174,969,892	174,968,689	−1203	0.719	0.781	0.062	2.092	0.676	0.753	0.077	0.017
22,901	17	ARSG	cg15308737	63,814,923	63,815,191	−268	0.820	0.879	0.059	2.090	0.817	0.853	0.036	0.055
140,685	20	BTBD4	cg21291985	61,907,479	61,907,300	−179	0.592	0.660	0.068	2.065	0.582	0.616	0.033	0.093
359	12	AQP2	cg12650635	48,630,730	48,630,796	−66	0.804	0.737	−0.066	2.054	0.796	0.773	−0.023	0.046
10,974	10	C10orf116	cg12261786	88,717,810	88,718,168	−358	0.426	0.377	−0.050	2.033	0.404	0.377	−0.027	0.006
2949	1	GSTM5	cg04987894	110,056,139	110,056,388	−249	0.1119	0.1685	0.0566	0.5664	0.1496	0.2330	0.0834	0.0335

List is ordered by NSDs of HCS samples. TSS, transcription start site; Chr, chromosome.

TABLE 4. A Total of 63 Genes With Exon Microarray Absolute Expression Change (FC) >1.25 in Both HCS and NDRI, and Bisulfite Microarray Sequencing Methylation Difference >2%

| | | | | | | | Expression | | | | |
| | | | | | | | HCS | | | | |
Gene ID	Chr	Symbol	CpG	CpG Location	TSS Coordinate	Distance to TSS	Control	AMD	AMD-Control	FC	NSD
15	17	AANAT	cg09382492	71,975,276	71,975,246	30	6.065	6.380	0.315	1.244	6.991
8038	10	ADAM12	cg13488201	128,067,313	128,067,055	−258	7.512	6.861	−0.652	−1.571	5.172
247	17	ALOX15B	cg15799267	7,883,131	7,883,127	4	6.418	6.932	0.514	1.428	0.641
23,452	9	ANGPTL2	cg11213150	128,924,278	128,924,865	587	7.586	7.175	−0.412	−1.330	9.087
314	17	AOC2	cg19317715	38,250,104	38,250,135	−31	5.799	6.849	1.049	2.070	0.833
10,930	6	APOBEC2	cg22375610	41,129,139	41,128,991	148	4.749	6.450	1.701	3.250	3.154
22,901	17	ARSG	cg15308737	63,814,923	63,815,191	−268	7.865	7.792	−0.072	−1.051	0.655
284,424	19	C19orf30	cg03996793	4,720,537	4,720,152	385	5.757	6.016	0.259	1.197	0.898
10,842	7	C7orf16	cg23216015	31,693,179	31,693,372	−193	5.561	5.717	0.156	1.115	1.139
389,799	9	C9orf171	cg25344672	134,275,028	134,275,432	−404	5.898	6.162	0.264	1.200	1.342
27,091	17	CACNG5	cg06226384	62,303,813	62,303,913	−100	5.926	6.857	0.931	1.906	4.184
283,316	12	CD163L1	cg13986618	7,487,248	7,488,015	767	6.769	6.400	−0.369	−1.292	1.348
1184	X	CLCN5	cg20062122	49,720,482	49,720,896	−414	7.999	7.677	−0.322	−1.250	0.638
119,587	10	CPXM2	cg09619146	125,641,024	125,641,490	466	9.596	9.303	−0.293	−1.225	0.628
1400	4	CRMP1	cg03544320	5,945,592	5,945,686	94	6.865	7.163	0.298	1.230	1.126
8451	13	CUL4A	cg16155588	112,909,934	112,911,087	−1153	7.789	7.510	−0.280	−1.214	5.573
54,849	16	DEF8	cg25193494	88,543,505	88,542,652	853	8.086	8.420	0.333	1.260	1.425
126,433	19	FBXO27	cg11402505	44,215,276	44,215,038	−238	7.318	7.882	0.564	1.478	2.439
26,157	7	GIMAP2	cg20663831	150,014,087	150,013,727	360	5.760	5.930	0.169	1.125	1.459
51,659	16	GINS2	cg19890739	84,281,040	84,280,081	−959	5.896	6.010	0.114	1.082	0.607
55,105	1	GPATCH2	cg01727899	215,872,498	215,871,032	−1466	7.782	7.446	−0.336	−1.262	4.095
390,212	11	GPR152	cg00587613	66,976,799	66,976,776	−23	6.655	6.966	0.311	1.241	2.311
9402	22	GRAP2	cg03840259	38,626,982	38,627,032	−50	6.862	6.208	−0.654	−1.574	3.604
2949	1	GSTM5	cg04987894	110,056,139	110,056,388	−249	9.389	8.444	−0.946	−1.926	2.102
3149	X	HMGB3	cg05935584	149,902,481	149,902,421	60	6.304	5.785	−0.519	−1.433	1.479
3624	7	INHBA	cg16415646	41,709,526	41,709,231	−295	6.375	6.790	0.416	1.334	5.121
3664	1	IRF6	cg23283495	208,046,402	208,046,102	−300	5.971	6.498	0.527	1.441	2.399
55,600	1	ITLN1	cg08356693	159,121,824	159,121,584	−240	3.566	3.718	0.153	1.112	1.386
199,834	1	LCE4A	cg17542385	150,948,603	150,948,176	427	5.804	6.322	0.518	1.432	3.224
84,856	10	LOC84856	cg00042156	42,290,848	42,290,967	−119	7.633	7.828	0.195	1.145	1.205
147,172	17	LRRC37B2	cg06488505	25,958,201	25,958,802	−601	6.213	6.374	0.161	1.118	1.452
2872	19	MKNK2	cg21030400	2,003,564	2,002,233	−1331	9.279	9.592	0.313	1.242	1.718
23,209	22	MLC1	cg05861567	48,865,813	48,866,041	228	6.762	7.026	0.264	1.201	1.667
4481	8	MSR1	cg01668126	16,095,111	16,094,595	−516	6.023	6.753	0.730	1.659	1.180
4481	8	MSR1	cg16303562	16,094,704	16,094,595	−109	6.023	6.753	0.730	1.659	1.180
4641	17	MYO1C	cg00597076	1,342,630	1,342,745	115	9.737	9.593	−0.144	−1.105	1.087
55,264	21	NA	cg13033054	32,870,432	32,870,062	−370	6.818	7.002	0.184	1.136	2.240
55,849	X	NA	cg19963797	110,811,123	110,811,069	54	4.242	4.080	−0.161	−1.118	1.175
4837	11	NNMT	cg14209518	113,671,846	113,671,745	101	7.739	8.395	0.655	1.575	1.085
26,532	19	OR10H3	cg25843439	15,713,574	15,713,203	371	5.922	5.218	−0.705	−1.630	2.782
5016	1	OVGP1	cg22997415	111,772,543	111,771,922	−621	6.261	6.016	−0.245	−1.185	2.707
9796	8	PHYHIP	cg05947740	22,145,723	22,145,549	−174	6.382	6.892	0.510	1.424	1.475
9271	12	PIWIL1	cg13861644	129,388,239	129,388,567	−328	5.519	5.138	−0.381	−1.302	2.035
5368	8	PNOC	cg03642518	28,230,922	28,230,568	354	6.377	6.577	0.200	1.149	1.945
5446	7	PON3	cg24750391	94,864,147	94,863,598	−549	7.154	6.277	−0.877	−1.836	1.329
5478	7	PPIA	cg17269548	44,802,815	44,802,777	38	6.990	6.808	−0.181	−1.134	0.996
5522	4	PPP2R2C	cg07867360	6,526,057	6,524,911	−1146	6.081	6.476	0.396	1.315	1.343
5935	X	RBM3	cg12251508	48,317,941	48,317,780	161	9.893	8.865	−1.028	−2.040	6.851
166,863	4	RBM46	cg22496683	155,922,060	155,921,950	110	5.157	4.750	−0.407	−1.326	1.006
27,316	X	RBMX	cg14642832	135,790,803	135,790,605	−198	7.708	7.907	0.199	1.148	1.090
55,511	X	SAGE1	cg19856594	134,803,587	134,803,451	136	3.323	3.438	0.115	1.083	3.568
65,012	12	SLC26A10	cg12883767	56,299,376	56,299,960	−584	6.590	6.338	−0.251	−1.190	0.866
6817	16	SULT1A1	cg18530748	28,542,345	28,542,367	22	7.438	7.196	−0.242	−1.183	2.310
6855	X	SYP	cg10818284	48,943,549	48,943,605	56	7.245	7.044	−0.201	−1.150	1.093
6872	X	TAF1	cg23986186	70,502,270	70,502,839	−569	8.135	8.003	−0.132	−1.096	6.151
84,218	17	TBC1D3F	cg14532417	33,601,782	33,602,396	614	3.271	6.520	3.248	9.503	8.660
79,875	15	THSD4	cg04616566	69,807,614	69,807,942	−328	8.330	7.995	−0.335	−1.262	1.852
11,011	17	TLK2	cg23181434	57,909,890	57,910,136	−246	6.464	6.142	−0.323	−1.251	0.994
6399	X	TRAPPC2	cg24352688	13,661,648	13,662,648	1000	4.961	4.689	−0.272	−1.208	1.076
10,346	11	TRIM22	cg12461141	5,667,230	5,667,664	−434	8.773	8.213	−0.560	−1.474	2.868
10,009	X	ZBTB33	cg13128531	119,268,412	119,268,635	−223	7.937	8.092	0.154	1.113	0.965
64,429	10	ZDHHC6	cg17872476	114,195,644	114,196,662	1018	7.956	7.574	−0.383	−1.304	2.066
7542	11	ZFPL1	cg19507591	64,606,853	64,608,270	−1417	8.253	8.387	0.134	1.097	1.316

Table is arranged alphabetically by gene symbol.

TABLE 4.   Extended

Expression					Methylation							
NDRI					HCS				NDRI			
Control	AMD	AMD-Control	FC	*P* Value	Control	AMD	AMD-Control	NSD	Control	AMD	AMD-Control	*P* Value
6.265	6.561	0.296	1.228	0.044	0.513	0.567	0.054	1.099	0.519	0.546	0.027	0.234
6.763	6.400	−0.363	−1.286	0.091	0.190	0.240	0.049	1.149	0.178	0.207	0.028	0.131
6.348	6.553	0.205	1.153	0.090	0.492	0.361	−0.131	4.936	0.411	0.387	−0.024	0.208
7.211	7.048	−0.163	−1.119	0.245	0.451	0.401	−0.050	0.945	0.413	0.377	−0.036	0.135
6.646	7.177	0.531	1.444	0.290	0.534	0.463	−0.071	1.127	0.506	0.482	−0.024	0.152
6.245	6.665	0.420	1.338	0.028	0.297	0.373	0.076	1.966	0.338	0.358	0.020	0.230
8.595	8.364	−0.231	−1.173	0.257	0.820	0.879	0.059	2.090	0.817	0.853	0.036	0.055
5.838	6.018	0.180	1.133	0.095	0.157	0.245	0.088	2.284	0.210	0.252	0.042	0.072
5.477	5.616	0.139	1.101	0.035	0.657	0.569	−0.088	0.535	0.649	0.613	−0.036	0.023
6.030	6.178	0.149	1.108	0.100	0.587	0.498	−0.089	5.956	0.549	0.522	−0.027	0.108
7.007	7.596	0.589	1.504	0.127	0.582	0.517	−0.065	1.466	0.577	0.554	−0.023	0.076
6.596	6.280	−0.316	−1.245	0.158	0.657	0.711	0.054	1.024	0.665	0.710	0.045	0.021
7.205	6.895	−0.310	−1.239	0.151	0.842	0.892	0.050	3.063	0.855	0.880	0.025	0.081
8.668	8.193	−0.476	−1.391	0.164	0.172	0.237	0.065	1.590	0.229	0.251	0.022	0.024
7.930	8.297	0.366	1.289	0.257	0.193	0.314	0.121	1.340	0.164	0.298	0.135	0.050
7.618	7.403	−0.215	−1.161	0.003	0.355	0.399	0.045	0.875	0.373	0.401	0.028	0.155
7.921	8.088	0.167	1.123	0.056	0.475	0.588	0.113	1.453	0.539	0.576	0.037	0.203
7.464	7.598	0.134	1.098	0.204	0.183	0.124	−0.059	3.000	0.155	0.130	−0.025	0.033
5.465	5.831	0.366	1.289	0.184	0.292	0.240	−0.052	1.139	0.362	0.332	−0.030	0.269
6.047	6.189	0.143	1.104	0.279	0.531	0.615	0.084	1.515	0.630	0.659	0.029	0.147
7.795	7.550	−0.244	−1.184	0.075	0.749	0.796	0.047	2.008	0.794	0.837	0.043	0.012
6.777	7.019	0.243	1.183	0.074	0.877	0.827	−0.050	3.051	0.857	0.837	−0.020	0.069
6.169	5.984	−0.185	−1.137	0.206	0.648	0.571	−0.077	1.078	0.621	0.602	−0.019	0.235
9.117	8.622	−0.495	−1.409	0.037	0.112	0.169	0.057	0.566	0.150	0.233	0.083	0.017
5.614	5.386	−0.228	−1.171	0.144	0.562	0.332	−0.231	0.707	0.284	0.251	−0.033	0.426
6.775	7.008	0.233	1.175	0.126	0.806	0.865	0.059	2.235	0.819	0.851	0.032	0.046
6.321	6.462	0.141	1.103	0.140	0.064	0.118	0.054	1.254	0.149	0.169	0.020	0.095
3.559	3.754	0.196	1.145	0.003	0.710	0.763	0.053	1.032	0.751	0.783	0.033	0.127
5.935	6.071	0.135	1.098	0.072	0.704	0.655	−0.049	1.222	0.662	0.637	−0.025	0.224
7.253	7.414	0.161	1.118	0.166	0.716	0.649	−0.066	1.345	0.647	0.597	−0.050	0.035
6.684	6.845	0.161	1.118	0.210	0.714	0.765	0.051	1.881	0.729	0.753	0.024	0.216
9.194	9.322	0.128	1.093	0.118	0.730	0.669	−0.060	0.673	0.741	0.682	−0.059	0.004
6.719	7.101	0.382	1.303	0.046	0.476	0.407	−0.070	1.094	0.508	0.490	−0.018	0.242
6.306	6.881	0.575	1.490	0.135	0.867	0.802	−0.065	6.126	0.859	0.836	−0.022	0.028
6.306	6.881	0.575	1.490	0.135	0.713	0.659	−0.053	0.752	0.714	0.696	−0.018	0.102
9.390	9.071	−0.319	−1.247	0.134	0.564	0.492	−0.073	2.492	0.596	0.578	−0.018	0.256
6.883	7.030	0.148	1.108	0.077	0.639	0.486	−0.154	2.903	0.538	0.509	−0.029	0.281
4.381	4.228	−0.153	−1.112	0.136	0.371	0.169	−0.201	1.317	0.168	0.131	−0.038	0.328
7.846	8.138	0.292	1.224	0.281	0.587	0.532	−0.055	1.457	0.582	0.557	−0.025	0.171
5.096	4.559	−0.537	−1.451	0.004	0.374	0.422	0.048	0.750	0.411	0.448	0.036	0.164
6.048	5.905	−0.143	−1.104	0.143	0.775	0.820	0.046	2.560	0.771	0.794	0.023	0.087
6.554	6.749	0.196	1.145	0.166	0.241	0.300	0.059	3.392	0.266	0.286	0.021	0.119
5.339	5.002	−0.337	−1.263	0.076	0.554	0.671	0.117	1.169	0.713	0.789	0.076	0.179
6.299	6.498	0.199	1.148	0.191	0.562	0.476	−0.086	1.840	0.534	0.504	−0.029	0.146
6.062	5.889	−0.174	−1.128	0.289	0.156	0.210	0.054	1.269	0.195	0.255	0.060	0.001
7.078	6.865	−0.213	−1.159	0.164	0.179	0.255	0.076	3.998	0.163	0.207	0.045	0.011
6.562	6.823	0.261	1.198	0.146	0.769	0.724	−0.045	1.292	0.778	0.744	−0.034	0.070
9.693	8.963	−0.730	−1.659	0.100	0.344	0.202	−0.142	0.840	0.174	0.154	−0.020	0.407
4.725	4.078	−0.647	−1.566	0.014	0.586	0.632	0.046	0.571	0.595	0.641	0.045	0.174
7.454	7.660	0.206	1.153	0.087	0.451	0.243	−0.208	0.895	0.209	0.185	−0.024	0.414
3.361	3.505	0.144	1.105	0.008	0.642	0.687	0.045	0.580	0.677	0.708	0.031	0.182
6.451	6.237	−0.214	−1.160	0.102	0.736	0.691	−0.045	0.987	0.767	0.745	−0.022	0.095
6.811	6.580	−0.231	−1.173	0.019	0.132	0.081	−0.051	3.120	0.117	0.092	−0.025	0.122
9.124	8.774	−0.350	−1.275	0.297	0.539	0.294	−0.245	0.811	0.255	0.237	−0.019	0.455
8.060	7.921	−0.139	−1.101	0.025	0.364	0.241	−0.124	2.505	0.258	0.229	−0.030	0.262
7.072	7.206	0.134	1.098	0.374	0.813	0.737	−0.076	3.492	0.783	0.751	−0.032	0.069
8.196	7.948	−0.247	−1.187	0.244	0.688	0.734	0.047	1.616	0.645	0.708	0.063	0.189
6.790	6.574	−0.216	−1.161	0.118	0.198	0.246	0.048	1.748	0.217	0.246	0.029	0.065
5.141	4.975	−0.166	−1.122	0.236	0.666	0.606	−0.061	0.673	0.596	0.576	−0.019	0.344
8.399	8.191	−0.208	−1.155	0.248	0.379	0.451	0.072	1.406	0.465	0.487	0.022	0.179
8.224	8.452	0.228	1.171	0.099	0.326	0.201	−0.125	0.995	0.190	0.167	−0.023	0.360
7.725	7.461	−0.263	−1.200	0.020	0.449	0.603	0.154	3.004	0.479	0.520	0.040	0.262
8.184	8.326	0.142	1.104	0.068	0.654	0.783	0.130	3.533	0.684	0.704	0.020	0.200

NSR
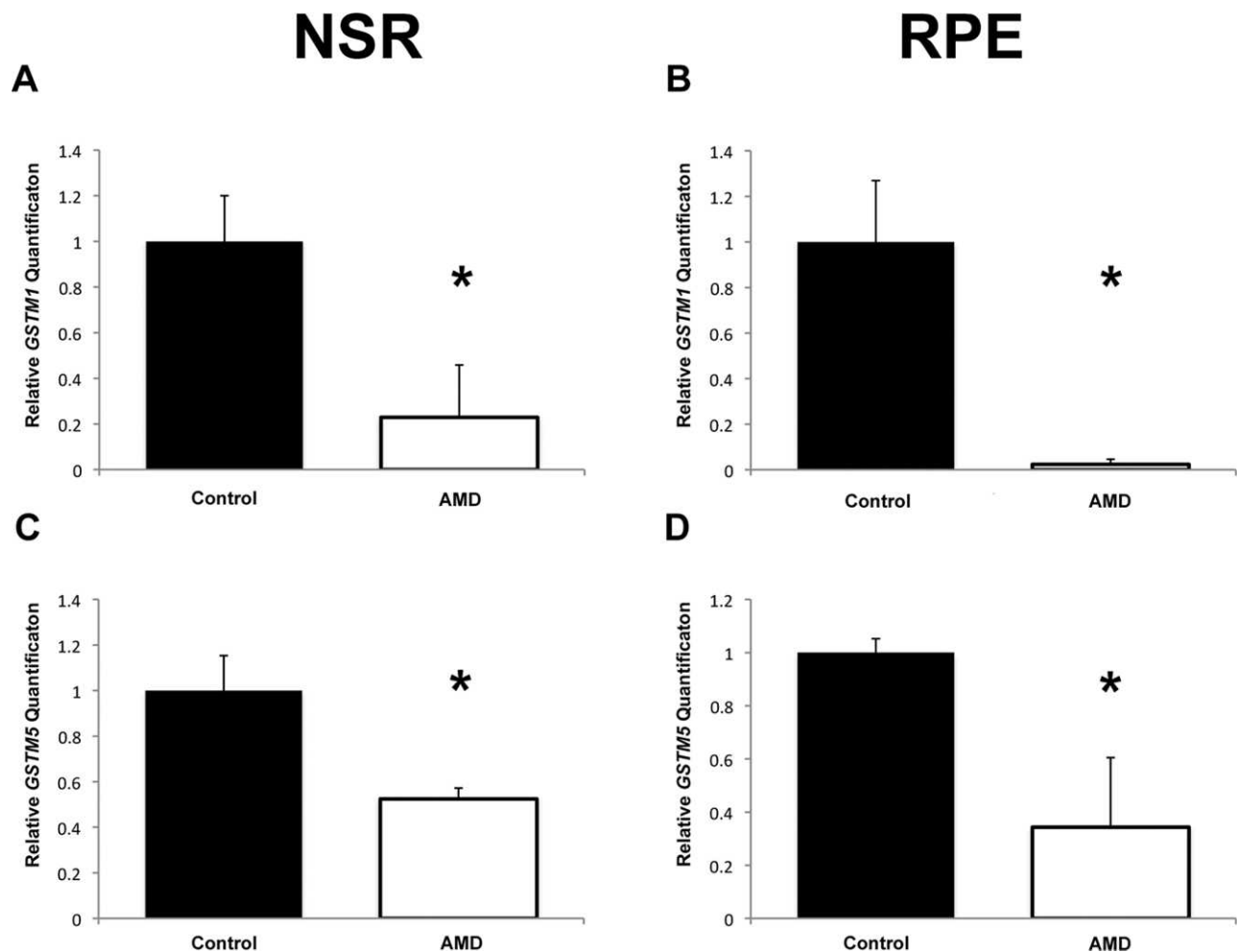
A

B

RPE

C

D

FIGURE 1. Graph showing relative quantification of *GSTM1* and *GSTM5* mRNA levels by qPCR in AMD versus controls. *GSTM1* mRNA levels were decreased in AMD samples in both NSR (**A**) and RPE (**B**) versus controls, *P* < 0.05 by two-sample *t*-test. *GSTM5* mRNA levels were decreased in both NSR (**C**) and RPE (**D**), *P* < 0.05.

available at http://www.iovs.org/lookup/suppl/doi:10.1167/iovs.11–8449/-/DCSupplemental). The FC and NSD between control and AMD were listed. Analysis was carried out on two separate groups of specimens and results sequentially compared. The first group was the HCS. These were classified as described previously (Supplemental Table 1).[47] The second set was from the NDRI, classified by medical history and confirmed by gross examination of the retina as described previously (Supplemental Table 1).[48] A total of 885 genes among the HCS eyes with FC and NSD greater than 25% and 3.0, respectively, were selected for comparison with NDRI samples. There were 46 genes with *P* values less than 0.1 and FC more than 25% (Table 1). The antioxidant gene *GSTM1* was reduced more than fivefold in AMD versus controls, whereas *GSTM5* was twofold reduced. Apolipoprotein B mRNA editing enzyme, catalytic polypeptide-like 2 (APOBEC2) was increased in AMD samples.

Quantitative PCR Confirmation of mRNA Levels

Most microarray exon expression results listed in Table 1 were confirmed by qPCR (Table 2). All relative expression changes (i.e., increased or decreased) as determined by exon microarray were confirmed by qPCR, except for 40S ribosomal protein S23 (RPS23, listed in bold type). Six genes tested by qPCR did not reach statistical significance for mRNA level changes.

Analysis of Promoter Methylation Determined by Bisulfite Microarray Sequencing in RPE/Choroid

Microarray analysis of AMD versus control RPE/choroid samples included 28,328 CpG dinucleotides spanning 14,495 genes; 561 CpG sites of HCS samples were selected with more than 5% difference in methylation (β value) in AMD versus control. This was compared with NDRI samples. Pearson correlation between HCS versus NDRI for the 561CpG sites was 0.229 (*P* = 4.3e[−8]). One sided *t*-test was applied to the 15 NDRI samples (Supplemental Table 4, available at http://www.iovs.org/lookup/suppl/doi:10.1167/iovs.11–8449/-/DCSupplemental) and 67 CpG sites with more than 5% methylation differences between AMD versus control were selected with *P* less than 0.1 (Table 3). *GSTM1* along with 2% of CpG sites were removed before any analysis owing to specimen-independent microarray platform read variation. CpG measurements of all RPE samples were further normalized by QSPLINE method using autosomal sites (Supplemental Table 4).

Stepwise Comparison of Methylation Changes Corresponding to Expression Changes in RPE Array Results

Microarray analysis comparing AMD versus control retinas indicate differences in RPE mRNA levels that corresponded to
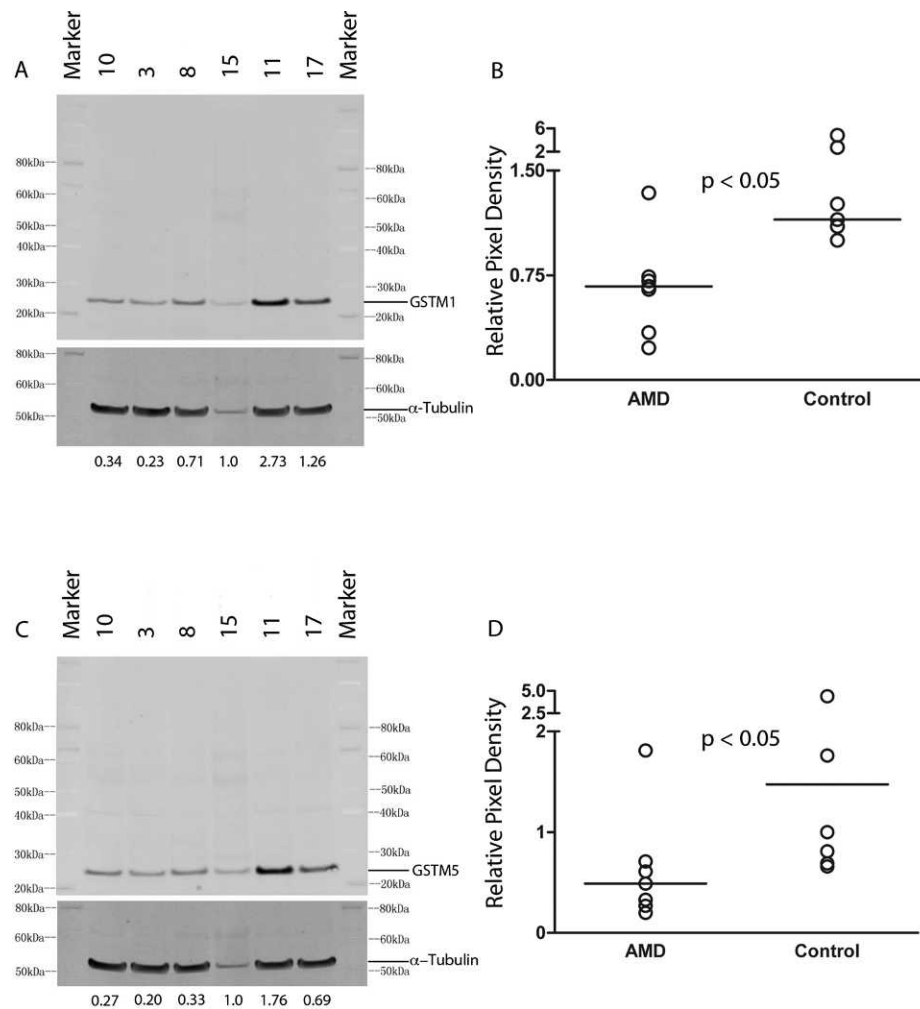
Figure 2. Western analysis of retinal NSR extracts from human samples. *GSTM1* levels were decreased in AMD versus control (**A**) with median levels of 0.67 vs. 1.15 (AMD versus control), total $n = 14$ (7 AMD versus 7 control) (**B**). *GSTM5* levels were decreased in AMD NSR (**C**) with median levels of 0.49 vs. 1.0 (AMD versus control), total $n = 14$ (**D**). Wilcoxon rank sum test was used because of the skewed distribution of data, $P < 0.05$.

methylation changes within the corresponding promoter sequences (Tables 1–3, Supplemental Tables 3 and 4). Genes were selected on the basis of an exon microarray NSD greater than 1.25 and a CpG methylation difference greater than 2% (Table 4). Of the possible 26,486 CpG-gene pairs, 63 genes were selected.

Reduced Levels of GSTM1 and GSTM5 mRNA Levels in AMD NSR and RPE/Choroid

Microarray analysis comparing the AMD versus control retinas suggested a possible difference in mRNA levels of *GSTM1* and *GSTM5*. This corresponded to hypermethylation of the promoter sequence of *GSTM5* (Table 4). qPCR was performed on all NSR and RPE samples from human postmortem specimens (Fig. 1). There was significantly less *GSTM1* and *GSTM5* mRNA in AMD eyes versus controls ($P < 0.05$).

Reduced GSTM1 and GSTM5 Protein in AMD Retinas

Western analysis of NSR was used to assess *GSTM1* and *GSTM5* protein levels in AMD ($n = 7$) versus controls ($n = 7$) (Fig. 2). A single band was detected with both anti-*GSTM1* and anti-

GSTM5 antibodies. Normalized to α-tubulin, the AMD eyes had a significant reduction in the amount of *GSTM1* and *GSTM5* ($P < 0.05$).

IHC Localization of GSTM1 and GSTM5

To assess retinal localization of *GSTM1* and *GSTM5,* control and AMD postmortem macular sections were immunostained. Sections were bleached before immunostaining to facilitate visualization of the immunolabel within the melanin-rich RPE (Fig. 3). In the normal and AMD retinas, *GSTM1* and *GSTM5* were present primarily within the apical aspect of RPE, the nerve fiber layer, the outer plexiform layer, and in the outer segments of the photoreceptors. Although IHC is semiquantitative at best, macula sections of AMD subjects had lighter immunostain in some RPE cells (Figs. 3E, 3H). Immunofluorescence detected similar *GSTM1* retinal localization in the albino mouse compared with human samples (Fig. 3F).

Bisulfite Pyrosequencing of GSTM1 and GSTM5 Promoter Confirm Hypermethylation of the GSTM1 Promoter

RPE *GSTM1* was significantly hypermethylated in AMD versus controls (Table 5). By comparing the methylation status of the
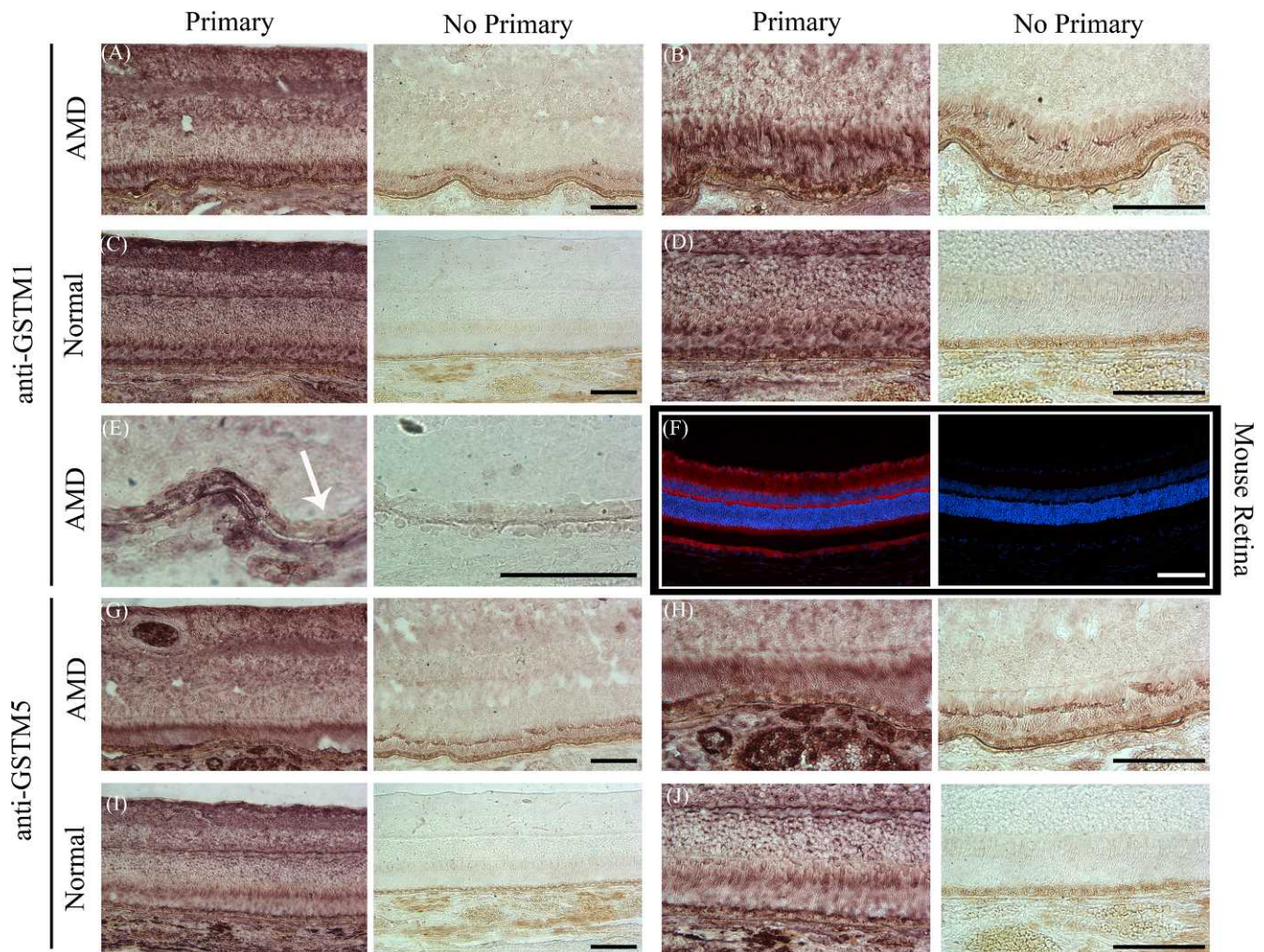
FIGURE 3. Photomicrographs of retina sections immunostained with either anti-GSTM1 or anti-GSTM5 antibodies. (**A**) *Left:* AMD retina immunostained with anti-GSTM1. *Right:* No primary antibody. (**B**) Higher magnification of A. (**C**) Normal human macula labeled with anti-GSTM1. (**D**) Higher magnification. (**E**) AMD retina labeled with anti-GSTM1 at higher magnification. Arrow shows diminished labeling intensity in RPE cells. (**F**) Albino Balb/c mouse retina stained with anti-GSTM1 (red fluorescence). Nuclei stained with DAPI (blue). (**G**) AMD retina immunostained with anti-GSTM5. (**H**) Higher magnification. (**I**) Normal human macula labeled with anti-GSTM5. (**J**) Higher magnification. Scale bar: 100 μm.

promoter to relative quantification of RPE mRNA for *GSTM1* and *GSTM5*, a significant correlation of total *GSTM1* promoter hypermethylation to decreased expression of both isoforms is evident (Table 6). NSR samples, in contrast, while showing a trend toward hypermethylation of *GSTM1* promoter in AMD, did not show a significant difference in total promoter methylation compared with controls (Table 5) and there did not appear to be a significant correlation of total NSR *GSTM1* promoter hypermethylation to decreased expression of either isoform, except in comparing maximum methylation percentage (Table 7).

There was no difference in total methylation of *GSTM5* promoter in AMD versus controls for NSR and RPE samples (Table 5). Total GSTM5 promoter methylation did not correlate with expression changes of that immediate downstream isoform (data not shown).

DISCUSSION

The gene expression pattern was altered in RPE/choroid of AMD versus control, as determined by exon microarray and confirmed for more than 20 genes by qPCR. Changes in the

percent methylation of specific cytosines within promoters of 63 genes with altered expression profiles were identified. *GSTM1* and *GSTM5* mRNA levels in NSR and RPE were decreased in postmortem AMD samples versus controls, and confirmed by qPCR (Fig. 1). RPE mRNA levels of each isoform were reduced to a greater extent than levels in NSR for AMD versus control. Similarly, there was a decrease of both protein isoforms in NSR extracts quantified by Western analysis (Fig. 2).

GST mu class was previously immunolocalized to Müller cells and rod outer segments in rats.[49] We found a similar distribution of *GSTM1* and *GSTM5* by immunohistochemistry in human retinas within the NSR and also detected both isoforms within the RPE (Fig. 3). *GSTM1* also localizes in the murine retinas in a similar manner (Fig. 3F).

Because there was a slight age-bias toward older patients in our AMD cohort (Supplemental Table 5, available at http://www.iovs.org/lookup/suppl/doi:10.1167/iovs.11–8449/-/DCSupplemental), we compared relative quantification of *GSTM1* and *GSTM5* mRNA levels to donor age and found no statistically significant age-dependent decline by both Pearson or Spearman correlation calculations (Supplemental Table 6, available at http://www.iovs.org/lookup/suppl/doi:10.1167/

TABLE 5. Comparison of Percent Methylation Data Between AMD and Controls: Comparison of Bisulfite Pyrosequencing Percent Methylation Average, Median, Maximum, and Minimum for *GSTM1* and *GSTM5* Promoter for NSR and RPE

	AMD Cases (*n* = 10)		Controls (*n* = 11)		
	n	Mean (SD)	*n*	Mean (SD)	*P* Value*
GSTM1 NSR					
CPG average	5	37.7 (5.07)	9	32.9 (7.91)	0.25
CPG median	5	35.4 (10.1)	9	28.0 (10.0)	0.21
CPG maximum	5	68.3 (7.07)	9	59.5 (15.7)	0.26
CPG minimum	5	8.22 (4.84)	9	10.1 (5.48)	0.53
GSTM1 RPE					
CPG average	10	22.9 (2.37)	10	16.2 (7.47)	**0.04**
CPG median	10	19.2 (5.88)	10	12.6 (7.67)	**0.04**
CPG maximum	10	38.6 (7.51)	10	31.1 (13.4)	0.14
CPG minimum	10	7.83 (3.72)	10	5.59 (3.79)	0.20
GSTM5 NSR					
CPG average	5	51.7 (3.11)	9	52.5 (3.02)	0.62
CPG median	5	53.2 (6.32)	9	54.3 (3.01)	0.72
CPG maximum	5	86.5 (4.44)	9	87.9 (6.09)	0.66
CPG minimum	5	16.4 (9.42)	9	18.0 (6.26)	0.70
GSTM5 RPE					
CPG average	10	22.4 (6.33)	10	25.7 (5.64)	0.24
CPG median	10	20.9 (6.38)	10	24.4 (5.75)	0.21
CPG maximum	10	48.8 (11.8)	10	50.8 (9.45)	0.68
CPG minimum	10	8.81 (2.96)	10	9.88 (4.58)	0.54

* From two-sample *t*-test of means.

TABLE 6. The Correlation Between RPE *GSTM1* Promoter Methylation and *GSTM1* and *GSTM5* Gene Expression: Pearson and Spearman Correlation of Percent Methylation (Individual CpG Dinucleotides, Average, Media, Maximum, and Minimum) and *GSTM1* and *GSTM5* Relative Gene Expression Determined by qPCR for RPE/Choroid

GSTM1 Methylation Location	Correlation Coefficient and *P* Value With *GSTM1* Gene Expression		Correlation Coefficient and *P* Value With *GSTM5* Gene Expression	
	Pearson Correlation	Spearman Correlation	Pearson Correlation	Spearman Correlation
CpG__1	−0.01669	−0.05904	−0.11474	−0.23509
	0.9443	0.8047	0.64	0.3326
CpG__2	−0.47005	−0.45366	−0.34243	−0.04386
	0.0365	**0.0445**	0.1513	0.8585
CpG__3	0.25108	0.21285	0.04744	−0.14035
	0.2856	0.3676	0.8471	0.5666
CpG__4	−0.38924	−0.53911	−0.1975	−0.06842
	0.0898	**0.0142**	0.4177	0.7808
CpG__5	−0.6437	−0.29363	−0.54658	−0.22807
	0.0022	0.2089	**0.0155**	0.3477
CpG__6	−0.58249	−0.2245	−0.53872	−0.29825
	0.007	0.3413	**0.0173**	0.2149
CpG__7	−0.22386	−0.07224	−0.33567	−0.56491
	0.3427	0.7621	0.16	**0.0117**
CpG__8	−0.53213	−0.42958	−0.59881	−0.63509
	0.0157	0.0587	**0.0067**	**0.0035**
CpG__9	−0.51406	−0.26256	−0.57479	−0.43333
	0.0204	0.2634	**0.01**	0.0638
CpG_average	−0.57789	−0.55464	−0.59848	−0.54386
	0.0076	**0.0111**	**0.0068**	**0.0161**
CpG_media	−0.40782	−0.47852	−0.45723	−0.58596
	0.0743	**0.0328**	**0.049**	**0.0084**
CpG_maximum	−0.5434	−0.49716	−0.44711	−0.08947
	0.0133	**0.0257**	0.0549	0.7157
CpG_minimum	−0.10095	−0.11186	−0.34811	−0.60351
	0.6719	0.6387	0.1442	**0.0062**

Significant *P* values are in bold.

TABLE 7. The Correlation Between NSR *GSTM1* Methylation and *GSTM1* and *GSTM5* Gene Expression: Pearson and Spearman Correlation of Percent Methylation (Individual Cpg Dinucleotides, Average, Media, Maximum, and Minimum) and *GSTM1* and *GSTM5* Relative Gene Expression Determined by qPCR for NSR

GSTM1 Methylation Location	Correlation Coefficient and *P* Value With *GSTM1* Gene Expression		Correlation Coefficient and *P* Value With *GSTM5* Gene Expression	
	Pearson Correlation	Spearman Correlation	Pearson Correlation	Spearman Correlation
CpG__1	0.08844	−0.56037	0.34053	0.13986
	0.796	0.073	0.2788	0.6646
CpG__2	−0.75036	−0.73349	−0.57685	−0.66434
	0.0078	**0.0102**	**0.0496**	**0.0185**
CpG__3	0.17865	−0.15034	0.30995	0.2662
	0.5992	0.659	0.3269	0.403
CpG__4	−0.47443	−0.60046	−0.25531	−0.59895
	0.1404	0.0508	0.4232	**0.0396**
CpG__5	−0.27526	−0.26879	−0.22223	−0.12587
	0.4127	0.4242	0.4876	0.6967
CpG__6	−0.24482	0.07289	−0.21525	0.04895
	0.4681	0.8313	0.5017	0.8799
CpG__7	0.38965	0.55125	0.26116	0.44755
	0.2362	0.0788	0.4123	0.1446
CpG__8	0.20985	0.1139	0.20004	0.23077
	0.5357	0.7388	0.5331	0.4705
CpG__9	−0.26344	−0.21868	−0.18274	−0.06993
	0.4338	0.5183	0.5697	0.829
CpG_average	−0.38165	−0.4328	−0.16966	−0.16783
	0.2468	0.1836	0.5981	0.6021
CpG_media	−0.30005	−0.48747	−0.04052	−0.00699
	0.37	0.1283	0.9005	0.9828
CpG_maximum	−0.5863	−0.6287	−0.49273	−0.59441
	0.058	**0.0383**	0.1036	**0.0415**
CpG_minimum	0.57967	0.48747	0.48633	0.51138
	0.0616	0.1283	0.1089	0.0893

Significant *P* values are in bold.

iovs.11–8449/-/DCSupplemental). The demographic characteristics of the samples used for protein quantification showed no significant difference in mean age or gender (Supplemental Table 7, available at http://www.iovs.org/lookup/suppl/doi:10.1167/iovs.11–8449/-/DCSupplemental). There was a Caucasian race predominance for all samples with only one sample being non-Caucasian, consistent with the higher prevalence of AMD in Caucasians.

DNA hypermethylation of the *GSTM1* promoter in RPE/choroid appears to coincide with diminished levels of both *GSTM1* and *GSTM5* transcripts. In addition to modulating expression of the adjoining gene, methylation of the *GSTM1* promoter may influence expression of the downstream gene, *GSTM5*. The *GSTM1* promoter may act as a CpG island shore for the downstream *GSTM5*.[33] Usually, these epigenetic changes occur without comitant genetic lesions (i.e., deletions or nulls).[35] If somatic mutation occurs at high frequency (i.e., adenomatosis polyposis coli in colorectal tumorigenesis), the promoter usually maintains a hypomethylated state. Additionally, epigenetic silencing is often an "early event" in the natural history of disease and hypermethylation of silent loci is observed before full-blown disease progression.[50–55] Epigenetic changes in plausible pathogenetic loci, therefore, are likely antecedent to disease "onset."

There are four known allelic variants of *GSTM1,* one of which is a deletion resulting in loss of function, which has been reported in up to 50% of the human population.[56,57] Information regarding allelic variants of the GSTMs is available in the ophthalmic literature.[58–63] In our sample set, we did not find any homozygous deletions for *GSTM1* (data not shown).

To increase the validity and minimize Poisson errors from our microarray analyses, we used two distinct sample cohorts. There was a modest correlation among microarray candidate genes listed in Tables 1 and 3 between HCS and NDRI sample sources. It is likely that a higher degree of statistical significance could have been obtained with a larger sample size and a larger cohort of histologically confirmed and staged AMD cases. The lack of histological classification in NDRI samples is a potential source of AMD misclassification and a limitation of the study.

The comparison of the expression exon microarray to the bisulfite DNA sequencing microarray data revealed 63 genes where methylation changes in promoter sequence correlated with changes in mRNA. Apolipoprotein B mRNA editing enzyme, APOBEC2, a member of the cytidine deaminase family of DNA/RNA editing enzymes, showed elevated transcription in RPE of AMD versus controls, which corresponded to hypermethylation. Increased methylation of promoter sequences are noted to cause elevated expression in certain "reduced-repressor" of promoter examples within the literature.[33] Hyperapolipoproteinemia B has been implicated in the pathogenesis of AMD in several human investigations and a recent description of an AMD-like transgenic murine model that hyperexpresses apoB100[64–67]; however, any effect of this mRNA editing enzyme on ApoB mRNA has not been elucidated.[68,69] APOBEC1, a cytidine deaminase family member, has been shown to "edit" APOB mRNA but the

physiologic role of APOBEC2 is still unknown.[70] Interestingly, APOBEC2 is induced by TGF-β signaling in a mammalian myoblastic cell line.[3,71] TGFβ has been shown to upregulate transcriptional factors associated with epithelial-mesenchymal transition in RPE cells in human choroidal neovascularization in AMD.[72]

We examined the relative quantification of mRNAs encoding several proteins involved in epigenetic modulation to determine if the changes in DNA methylation in AMD were attributable to a more generalized disruption of epigenetic mechanisms. mRNAs of MBD1-3 proteins, methyl CpG binding protein 2, an MBD gene family member, tRNA aspartic acid methyltransferase, histone acetyltransferase, HDAC, and histamine N-methyltransferase were not significantly different in AMD versus control (Table 2, bottom). This suggests that the hypermethylation of the *GSTM1* promoter in AMD is not a result of a global dysfunction or loss of function of epigenetic control mechanisms within the retina.

Retinal GSTs are likely to have a significant role in protection against oxidative insult.[36,73–80] Pharmacologic augmentation of the body's antioxidant defenses, therefore, may prove to be protective in AMD pathogenesis, especially in people with low *GSTM1* and *GSTM5* expression.

In conclusion, we report here the first evidence of a potential decrease of specific *GSTM* isoenzymes in human postmortem ophthalmic specimens in relation to a retinal disease, AMD. The function and location of these isoenzymes suggest that this decline in antioxidant function could lead to increased oxidative stress in AMD eyes and contribute to AMD pathogenesis. The hypermethylation of the *GSTM1* promoter coincides with diminished expression of two immediate downstream genes, *GSTM1* and *GSTM5*, suggesting that these methylation events could contribute to AMD risk or pathogenesis.

References

1. Gaillard ER, Atherton SJ, Eldred G, Dillon J. Photophysical studies on human retinal lipofuscin. *Photochem Photobiol*. 1995;61:448–453.

2. Rozanowska M, Jarvis-Evans J, Korytowski W, Boulton ME, Burke JM, Sarna T. Blue light-induced reactivity of retinal age pigment. In vitro generation of oxygen-reactive species. *J Biol Chem*. 1995;270:18825–18830.

3. Martinez-Lara E, Siles E, Hernandez R, et al. Glutathione S-transferase isoenzymatic response to aging in rat cerebral cortex and cerebellum. *Neurobiol Aging*. 2003;24:501–509.

4. Beatty S, Koh H, Phil M, Henson D, Boulton M. The role of oxidative stress in the pathogenesis of age-related macular degeneration. *Surv Ophthalmol*. 2000;45:115–134.

5. Mirza S, Plafker KS, Aston C, Plafker SM. Expression and distribution of the class III ubiquitin-conjugating enzymes in the retina. *Mol Vis*. 2010;16:2425–2437.

6. Halliwell B, Gutteridge JM. Oxygen toxicity, oxygen radicals, transition metals and disease. *Biochem J*. 1984;219:1–14.

7. Peinado MA, Quesada A, Pedrosa JA, et al. Light microscopic quantification of morphological changes during aging in neurons and glia of the rat parietal cortex. *Anat Rec*. 1997; 247:420–425.

8. Sies H. Oxidative stress: from basic research to clinical application. *Am J Med*. 1991;91:31S–38S.

9. Yu BP. Cellular defenses against damage from reactive oxygen species. *Physiol Rev*. 1994;74:139–162.

10. A randomized, placebo-controlled, clinical trial of high-dose supplementation with vitamins C and E, beta carotene, and zinc for age-related macular degeneration and vision loss: AREDS report no. 8. *Arch Ophthalmol* 2001;119:1417–1436.

11. Organisciak DT, Bicknell IR, Darrow RM. The effects of L-and D-ascorbic acid administration on retinal tissue levels and light damage in rats. *Curr Eye Res*. 1992;11:231–241.

12. Petrova LI, Molodova GA, Burtseva NN. Conditions of dextranase formation by *Penicillium funiculosum* 15 [in Russian]. *Prikl Biokhim Mikrobiol*. 1975;11:63–66.

13. Garcia-Castineiras S, Velazquez S, Martinez P, Torres N. Aqueous humor hydrogen peroxide analysis with dichloro-phenol-indophenol. *Exp Eye Res*. 1992;55:9–19.

14. Spector A, Ma W, Wang RR. The aqueous humor is capable of generating and degrading H2O2. *Invest Ophthalmol Vis Sci*. 1998;39:1188–1197.

15. Crabb JW, Miyagi M, Gu X, et al. Drusen proteome analysis: an approach to the etiology of age-related macular degeneration. *Proc Natl Acad Sci U S A*. 2002;99:14682–14687.

16. Gu X, Meer SG, Miyagi M, et al. Carboxyethylpyrrole protein adducts and autoantibodies, biomarkers for age-related macular degeneration. *J Biol Chem*. 2003;278:42027–42035.

17. Ates O, Azizi S, Alp HH, et al. Decreased serum paraoxonase 1 activity and increased serum homocysteine and malondialdehyde levels in age-related macular degeneration. *Tohoku J Exp Med*. 2009;217:17–22.

18. Friedman DS, O'Colmain BJ, Munoz B, et al. Prevalence of age-related macular degeneration in the United States. *Arch Ophthalmol*. 2004;122:564–572.

19. Buch H, Vinding T, la Cour M, Jensen GB, Prause JU, Nielsen NV. Risk factors for age-related maculopathy in a 14-year follow-up study: the Copenhagen City Eye Study. *Acta Ophthalmol Scand*. 2005;83:409–418.

20. Smith W, Assink J, Klein R, et al. Risk factors for age-related macular degeneration: pooled findings from three continents. *Ophthalmology*. 2001;108:697–704.

21. Frederick JM, Rayborn ME, Laties AM, Lam DM, Hollyfield JG. Dopaminergic neurons in the human retina. *J Comp Neurol*. 1982;210:65–79.

22. Hyman LG, Lilienfeld AM, Ferris FL 3rd, Fine SL. Senile macular degeneration: a case-control study. *Am J Epidemiol*. 1983;118: 213–227.

23. Valko M, Rhodes CJ, Moncol J, Izakovic M, Mazur M. Free radicals, metals and antioxidants in oxidative stress-induced cancer. *Chem Biol Interact*. 2006;160:1–40.

24. Valko M, Izakovic M, Mazur M, Rhodes CJ, Telser J. Role of oxygen radicals in DNA damage and cancer incidence. *Mol Cell Biochem*. 2004;266:37–56.

25. Wachsman JT. DNA methylation and the association between genetic and epigenetic changes: relation to carcinogenesis. *Mutat Res*. 1997;375:1–8.

26. Lim SO, Gu JM, Kim MS, et al. Epigenetic changes induced by reactive oxygen species in hepatocellular carcinoma: methylation of the E-cadherin promoter. *Gastroenterology*. 2008;135: 2128–2140. 2140 e2121-2128.

27. Valinluck V, Tsai HH, Rogstad DK, Burdzy A, Bird A, Sowers LC. Oxidative damage to methyl-CpG sequences inhibits the binding of the methyl-CpG binding domain (MBD) of methyl-CpG binding protein 2 (MeCP2). *Nucleic Acids Res*. 2004;32: 4100–4108.

28. Zhu WG, Srinivasan K, Dai Z, et al. Methylation of adjacent CpG sites affects Sp1/Sp3 binding and activity in the p21(Cip1) promoter. *Mol Cell Biol*. 2003;23:4056–4065.

29. Jones PA. DNA methylation and cancer. *Oncogene*. 2002;21: 5358–5360.

30. Robertson KD. DNA methylation and human disease. *Nat Rev Genetics*. 2005;6:597–610.

31. Wilson AS, Power BE, Molloy PL. DNA hypomethylation and human diseases. *Biochim Biophys Acta*. 2007;1775:138–162.

32. Baylin SB, Ohm JE. Epigenetic gene silencing in cancer—a mechanism for early oncogenic pathway addiction? *Nat Rev Cancer*. 2006;6:107–116.

33. Doi A, Park IH, Wen B, et al. Differential methylation of tissue- and cancer-specific CpG island shores distinguishes human induced pluripotent stem cells, embryonic stem cells and fibroblasts. *Nat Genet*. 2009;41:1350–1353.

34. Herman JG, Baylin SB. Gene silencing in cancer in association with promoter hypermethylation. *N Engl J Med*. 2003;349: 2042–2054.

35. Esteller M, Corn PG, Baylin SB, Herman JG. A gene hyper-methylation profile of human cancer. *Cancer Res*. 2001;61: 3225–3229.

36. Joshi PM, Franco M, Dubovy S, Bhattacharya SK, Lee WH. Decreased expression of GSTP1 in the macula leads to AMD pathogenesis. *Invest Ophthalmol Vis Sci*. 2009:poster 2346/D1079.

37. Jones PA, Laird PW. Cancer epigenetics comes of age. *Nat Genet*. 1999;21:163–167.

38. Baylin SB, Herman JG. DNA hypermethylation in tumorigenesis: epigenetics joins genetics. *Trends Genet*. 2000;16:168–174.

39. Fang MZ, Wang Y, Ai N, et al. Tea polyphenol (-)-epigallocatechin-3-gallate inhibits DNA methyltransferase and reactivates methylation-silenced genes in cancer cell lines. *Cancer Res*. 2003;63:7563–7570.

40. McLarty J, Bigelow RL, Smith M, Elmajian D, Ankem M, Cardelli JA. Tea polyphenols decrease serum levels of prostate-specific antigen, hepatocyte growth factor, and vascular endothelial growth factor in prostate cancer patients and inhibit production of hepatocyte growth factor and vascular endothelial growth factor in vitro. *Cancer Prev Res (Phila)*. 2009;2: 673–682.

41. Aggarwal BB. Prostate cancer and curcumin: add spice to your life. *Cancer Biol Ther*. 2008;7:1436–1440.

42. Pandey M, Shukla S, Gupta S. Promoter demethylation and chromatin remodeling by green tea polyphenols leads to re-expression of GSTP1 in human prostate cancer cells. *Int J Cancer*. 2010;126:2520–2533.

43. Seddon JM, Reynolds R, Shah HR, Rosner B. Smoking, dietary betaine, methionine, and vitamin D in monozygotic twins with discordant macular degeneration: epigenetic implications. *Ophthalmology*. 2011;118:1386–1394.

44. Hadziahmetovic M, Song Y, Ponnuru P, et al. Age-dependent retinal iron accumulation and degeneration in hepcidin knockout mice. *Invest Ophthalmol Vis Sci*. 2011;52:109–118.

45. Dunaief JL, Dentchev T, Ying GS, Milam AH. The role of apoptosis in age-related macular degeneration. *Arch Ophthalmol*. 2002;120:1435–1442.

46. Gnana-Prakasam JP, Martin PM, Mysona BA, Roon P, Smith SB, Ganapathy V. Hepcidin expression in mouse retina and its regulation via lipopolysaccharide/Toll-like receptor-4 pathway independent of Hfe. *Biochem J*. 2008;411:79–88.

47. Curcio CA, Medeiros NE, Millican CL. The Alabama Age-Related Macular Degeneration Grading System for donor eyes. *Invest Ophthalmol Vis Sci*. 1998;39:1085–1096.

48. Chowers I, Wong R, Dentchev T, et al. The iron carrier transferrin is upregulated in retinas from patients with age-related macular degeneration. *Invest Ophthalmol Vis Sci*. 2006;47:2135–2140.

49. McGuire S, Daggett D, Bostad E, Schroeder S, Siegel F, Kornguth S. Cellular localization of glutathione S-transferases in retinas of control and lead-treated rats. *Invest Ophthalmol Vis Sci*. 1996;37:833–842.

50. Dvorak K, Payne CM, Chavarria M, et al. Bile acids in combination with low pH induce oxidative stress and oxidative DNA damage: relevance to the pathogenesis of Barrett's oesophagus. *Gut*. 2007;56:763–771.

51. Salinas AE, Wong MG. Glutathione S-transferases—a review. *Curr Med Chem*. 1999;6:279–309.

52. Strange RC, Spiteri MA, Ramachandran S, Fryer AA. Glutathione-S-transferase family of enzymes. *Mutat Res*. 2001;482:21–26.

53. Issa JP, Ahuja N, Toyota M, Bronner MP, Brentnall TA. Accelerated age-related CpG island methylation in ulcerative colitis. *Cancer Res*. 2001;61:3573–3577.

54. Peng DF, Kanai Y, Sawada M, et al. DNA methylation of multiple tumor-related genes in association with overexpression of DNA methyltransferase 1 (DNMT1) during multistage carcinogenesis of the pancreas. *Carcinogenesis*. 2006;27: 1160–1168.

55. Yu K, Zhuang J, Kaminski JM, et al. CXCR4 down-regulation by small interfering RNA inhibits invasion and tubule formation of human retinal microvascular endothelial cells. *Biochem Biophys Res Commun*. 2007;358:990–996.

56. Nakajima T, Elovaara E, Anttila S, et al. Expression and polymorphism of glutathione S-transferase in human lungs: risk factors in smoking-related lung cancer. *Carcinogenesis*. 1995;16:707–711.

57. Strange RC, Jones PW, Fryer AA. Glutathione S-transferase: genetics and role in toxicology. *Toxicol Lett*. 2000;112–113: 357–363.

58. Jourenkova-Mironova N, Voho A, Bouchardy C, et al. Glutathione S-transferase GSTM3 and GSTP1 genotypes and larynx cancer risk. *Cancer Epidemiol Biomarkers Prev*. 1999; 8:185–188.

59. Jourenkova N, Reinikainen M, Bouchardy C, Dayer P, Benhamou S, Hirvonen A. Larynx cancer risk in relation to glutathione S-transferase M1 and T1 genotypes and tobacco smoking. *Cancer Epidemiol Biomarkers Prev*. 1998;7:19–23.

60. Jahnke V, Matthias C, Fryer A, Strange R. Glutathione S-transferase and cytochrome-P-450 polymorphism as risk factors for squamous cell carcinoma of the larynx. *Am J Surg*. 1996;172:671–673.

61. Lafuente A, Pujol F, Carretero P, Villa JP, Cuchi A. Human glutathione S-transferase mu (GST mu) deficiency as a marker for the susceptibility to bladder and larynx cancer among smokers. *Cancer Lett*. 1993;68:49–54.

62. Olshan AF, Weissler MC, Watson MA, Bell DA. GSTM1, GSTT1, GSTP1, CYP1A1, and NAT1 polymorphisms, tobacco use, and the risk of head and neck cancer. *Cancer Epidemiol Biomarkers Prev*. 2000;9:185–191.

63. Kihara M, Kihara M, Kubota A, Furukawa M, Kimura H. GSTM1 gene polymorphism as a possible marker for susceptibility to head and neck cancers among Japanese smokers. *Cancer Lett*. 1997;112:257–262.

64. Colak E, Kosanovic-Jakovic N, Zoric L, Radosavljevic A, Stankovic S, Majkic-Singh N. The association of lipoprotein parameters and C-reactive protein in patients with age-related macular degeneration. *Ophthalmic Res*. 2011;46:125–132.

65. Fujihara M, Bartels E, Nielsen LB, Handa JT. A human apoB100 transgenic mouse expresses human apoB100 in the RPE and develops features of early AMD. *Exp Eye Res*. 2009;88:1115–1123.

66. Sallo FB, Bereczki E, Csont T, et al. Bruch's membrane changes in transgenic mice overexpressing the human biglycan and apolipoprotein b-100 genes. *Exp Eye Res*. 2009;89:178–186.

67. Nowak M, Swietochowska E, Marek B, et al. Changes in lipid metabolism in women with age-related macular degeneration. *Clin Exp Med*. 2005;4:183–187.

68. Prochnow C, Bransteitter R, Klein MG, Goodman MF, Chen XS. The APOBEC-2 crystal structure and functional implications for the deaminase AID. *Nature*. 2007;445:447–451.

69. Etard C, Roostalu U, Strahle U. Lack of Apobec2-related proteins causes a dystrophic muscle phenotype in zebrafish embryos. *J Cell Biol*. 2010;189:527–539.

70. Harjes E, Gross PJ, Chen KM, et al. An extended structure of the APOBEC3G catalytic domain suggests a unique holoenzyme model. *J Mol Biol*. 2009;389:819–832.

71. Vonica A, Rosa A, Arduini BL, Brivanlou AH. APOBEC2, a selective inhibitor of TGFbeta signaling, regulates left-right axis specification during early embryogenesis. *Dev Biol*. 2011; 350:13–23.

72. Hirasawa M, Noda K, Noda S, et al. Transcriptional factors associated with epithelial-mesenchymal transition in choroidal neovascularization. *Mol Vis*. 2011;17:1222–1230.

73. Keys SA, Zimmerman WF. Antioxidant activity of retinol, glutathione, and taurine in bovine photoreceptor cell membranes. *Exp Eye Res*. 1999;68:693–702.

74. Balin AK, Allen RG. Mechanisms of biologic aging. *Dermatol Clin*. 1986;4:347–358.

75. Singh SV, Dao DD, Srivastava SK, Awasthi YC. Purification and characterization of glutathione S-transferases in human retina. *Curr Eye Res*. 1984;3:1273–1280.

76. De La Paz MA, Zhang J, Fridovich I. Red blood cell antioxidant enzymes in age-related macular degeneration. *Br J Ophthalmol*. 1996;80:445–450.

77. Nicolas MG, Fujiki K, Murayama K, et al. Studies on the mechanism of early onset macular degeneration in cynomolgus monkeys. II. Suppression of metallothionein synthesis in the retina in oxidative stress. *Exp Eye Res*. 1996;62:399–408.

78. Cohen SM, Olin KL, Feuer WJ, Hjelmeland L, Keen CL, Morse LS. Low glutathione reductase and peroxidase activity in age-related macular degeneration. *Br J Ophthalmol*. 1994;78:791–794.

79. Sheehan D, Meade G, Foley VM, Dowd CA. Structure, function and evolution of glutathione transferases: implications for classification of non-mammalian members of an ancient enzyme superfamily. *Biochem J*. 2001;360:1–16.

80. Rebbeck TR. Molecular epidemiology of the human glutathione S-transferase genotypes GSTM1 and GSTT1 in cancer susceptibility. *Cancer Epidemiol Biomarkers Prev*. 1997;6: 733–743.